Postsynaptic Abnormalities at the Neuromuscular Junctions of Utrophin-deficient Mice

Anne E. Deconinck,* Allyson C. Potter,* Jonathon M. Tinsley,* Sarah J. Wood,‡ Ruth Vater,‡ Carol Young,‡ Laurent Metzinger,* Angela Vincent,§ Clarke R. Slater,‡ and Kay E. Davies*

*Laboratory of Genetics, Department of Biochemistry, University of Oxford, South Parks Road, Oxford OX1 3QU, United Kingdom; ‡School of Neurosciences, University of Newcastle upon Tyne and Muscular Dystrophy Group Research Laboratories, Newcastle General Hospital, Newcastle upon Tyne NE4 6BE, United Kingdom; and §Neurosciences Group, Institute of Molecular Medicine, John Radcliffe Hospital, Oxford OX3 9QU, United Kingdom

Abstract. Utrophin is a dystrophin-related cytoskeletal protein expressed in many tissues. It is thought to link F-actin in the internal cytoskeleton to a transmembrane protein complex similar to the dystrophin protein complex (DPC). At the adult neuromuscular junction (NMJ), utrophin is precisely colocalized with acetylcholine receptors (AChRs) and recent studies have suggested a role for utrophin in AChR cluster formation or maintenance during NMJ differentiation. We have disrupted utrophin expression by gene targeting in the mouse. Such mice have no utrophin detectable by Western blotting or immunocytochemistry. Utrophin-deficient mice are healthy and show no signs of weakness. However, their NMJs have reduced numbers of AChRs (α-bungarotoxin [α-BgTx] binding reduced to ~60% normal) and decreased postsynaptic folding, though only minimal electrophysiological changes. Utrophin is thus not essential for AChR clustering at the NMJ but may act as a component of the postsynaptic cytoskeleton, contributing to the development or maintenance of the postsynaptic folds. Defects of utrophin could underlie some forms of congenital myasthenic syndrome in which a reduction of postsynaptic folds is observed.

Utrophin is a component of the membrane cytoskeleton, found in many tissues. It is a close homologue of dystrophin (reviewed in Blake et al., 1996), which causes the severe muscle wasting disease in man, Duchenne muscular dystrophy (Hoffman et al., 1987; Koenig et al., 1988). Both proteins are thought to link the internal cytoskeleton of the muscle cell to the extracellular matrix (reviewed in Ahn and Kunkel, 1993; Tinsley et al., 1994; Campbell et al., 1995). The NH_2-terminal region of dystrophin binds F-actin while the COOH-terminal region binds to β-dystroglycan, a component of the dystrophin protein complex (DPC)[1] (Ervasti et al., 1990; Ervasti and Campbell, 1991; Ibraghimov-Beskrovnaya, 1992). α-Dystroglycan, a further component of the DPC, is thought to bind to laminin in the extracellular matrix (Ohlendieck and Campbell, 1991; Dickson et al., 1992; Ervasti and Campbell, 1993). Utrophin shares 85% amino acid conservation with dystrophin in the NH_2- and COOH-terminal regions (Love et al., 1989; Tinsley et al., 1992) and is likely to have similar binding partners (Matsumura et al., 1992; Winder et al., 1995; Winder and Kendrick-Jones, 1995; James et al., 1996).

Unlike dystrophin, which is only expressed in muscle and brain in the adult, utrophin is expressed in a wide variety of adult tissues. The presence of utrophin in vascular smooth muscle and the endothelium appears to underlie its very general tissue distribution with highest levels of protein and mRNA expression in lung and kidney (Love et al., 1989, 1991; Schofield et al., 1993). Utrophin appears early in the development of the mouse with the first transcripts detectable in the neural groove at embryonic day 8.5 (Schofield et al., 1993). Subsequent utrophin expression is particularly abundant in a subset of tissues derived from the neural crest such as peripheral nerve where it colocalizes with dystroglycan and homologues of other dystrophin-associated proteins (Matsumura et al., 1993).

In many tissues and cultured cells, utrophin is present at specialized cell–cell or cell–extracellular matrix contacts. These include the foot processes of the kidney filtration barrier, the bronchial wall of the alveoli, and the intercalated discs of the heart (Pons et al., 1994) as well as focal adhesions and adherens-type junctions (Belkin et al., 1994; Belkin and Burridge, 1995). In brain, in addition to its en-

Please address all correspondence to K.E. Davies, Laboratory of Genetics, Department of Biochemistry, University of Oxford, South Parks Road, Oxford OX1 3QU, United Kingdom. Tel.: 44 1865 275324. Fax: 44 1865 275215.

1. *Abbreviations used in this paper*: AChE, acetylcholinesterase; AChR, acetylcholine receptor; α-BgTx, α-bungarotoxin; DIA, diaphragm; DPC, dystrophin protein complex; EDL, *extensor digitorum longus*; ETA, *epitrochleoanconeus*; NMJ, neuromuscular junction; SOL, *soleus.*

richment in vascularized regions and in the astrocyte foot processes of the blood-brain barrier (Khurana et al., 1992), utrophin is reported to be present in the postsynaptic region of some synapses (Kamakura et al., 1994). In adult skeletal muscle fibers, in contrast to dystrophin, utrophin is present only at the neuromuscular junction (NMJ) and the myotendinous junction (Ohlendieck et al., 1991; Nguyen thi Man et al., 1991; Bewick et al., 1992), although a more general distribution is found in embryonic and regenerating muscle (Khurana et al., 1991; Helliwell et al., 1992; Karpati et al., 1993; Koga et al., 1993; Sewry et al., 1994).

The NMJ is a cell–cell junction where utrophin is normally associated with an essential ligand-gated ion channel, the acetylcholine receptor (AChR). The postsynaptic membrane of the NMJ is characterized by extensive folding. Utrophin precisely colocalizes with the AChRs at the crests and upper part of these folds, while dystrophin and β-spectrin are concentrated with voltage-gated sodium channels in the depths of the folds (Flucher and Daniels, 1989; Bewick et al., 1992; Sealock et al., 1991). This colocalization of utrophin and AChRs is present in the embryo from the earliest stage of AChR clustering and throughout the postnatal maturation of the NMJ (Phillips et al., 1993; Bewick et al., 1996) as is rapsyn, a NMJ-specific protein known to be essential in AChR clustering (Froehner et al., 1990; Phillips et al., 1991; Gautam et al., 1995). In contrast, dystrophin and spectrin do not appear at the NMJ until well after AChR clusters have formed (Bewick et al., 1996). Further evidence for a link between utrophin and the AChRs comes from the finding that utrophin is greatly reduced at the NMJ in some acquired and inherited AChR deficiencies in man whereas dystrophin and several other postsynaptic proteins are not (Slater et al., 1994). Finally, in addition to its synapse-specific location in muscle cells, expression of the utrophin gene may also be controlled by synapse-specific factors. The promoter region of utrophin has recently been found to contain an N-box motif, which is also present in the genes for the δ subunit of the AChR and β2-syntrophin which are preferentially expressed at the NMJ (Dennis et al., 1996).

The pattern of expression of utrophin suggests that it may be involved in the development and maintenance of a wide variety of tissues. The large size of the utrophin gene, like that of dystrophin, makes it a likely candidate for natural mutation (Pearce et al., 1993). Nonetheless, no naturally occurring diseases of man or animals have been identified as resulting from mutations of the utrophin gene, possibly because such mutations are always lethal. To investigate the function of utrophin, we therefore created mice with a null mutation in the utrophin gene. We focused much of our attention on characterizing the effects of the lack of utrophin on the properties of the NMJ.

Materials and Methods

Gene Targeting Construct

Restriction and modifying enzymes were used following the manufacturer's instructions (Boehringer Mannheim, Lewes, UK or Biolabs). Radioactive label was obtained from Amersham International (Amersham, UK) or ICN (Thane, UK). The 129/Sv library (kindly donated by Terry Rabbitts, Cambridge, UK) was screened using a 5′-end human utrophin cDNA clone (89.2; Tinsley et al., 1992). A 7-kb EcoRI fragment comprising a single exon flanked by 3.5 kb of isogenic DNA on either side was subcloned into pUC18. A 1-kb genomic EcoRI–EcoRV fragment located at the 5′-end was subsequently removed for use as an external probe and the remaining fragment was subcloned into pBluescript II SK− (Stratagene, La Jolla, CA). A neomycin resistance cassette (neo) driven by the phosphoglycerate kinase-1 (pgk) promoter was introduced into the EcoRV site in the exon. 40 μg of targeting construct was released from vector backbone by BamHI digestion and purified by gel electrophoresis and Qiagen extraction before electroporation.

Transfection of R1 ES Cells and Generation of *utrn*−/− Mice

Methods were essentially those of Wurst and Joyner (1993) and Papaioannou and Johnson (1993). ES cells (R1 ES cell line was kindly donated by Andras Nagy, Mount Sinai Hospital, Toronto, Canada) were routinely passaged on monolayers of mitotically inactivated primary embryonic fibroblast cells (made from CD1 mice) in ES cell culture medium (all Gibco). 5×10^6 ES cells were electroporated in 0.4-cm cuvettes in a Biorad Gene Pulser at 0.34 kV/250 μF or 0.25 kV/500 μF. Transfected cells were selected in ES cell medium containing 300 μg/ml G418 (Gibco). G418 resistant colonies were cloned in 96-well plates and DNA prepared for BamHI digestion. Correct targeting events were identified by Southern blot analysis using the 5′ flanking probe and the internal neo probe. Two targeted clones were injected into 3.5-d-old C57BL6 blastocysts which were transferred into ICR pseudopregnant females. 12 chimeras were generated, of which 10 were male, all with ~95% coat color chimerism. These were mated to DBA/C57 F1 females; 6 produced agouti offspring at a high percentage (being germline transmission of the mutated ES cells). Southern blotting of genomic DNA from tail biopsies was used to identify heterozygotes (*Utrn*+/−), which were mated to produce homozygous offspring (*Utrn*−/−).

RT-PCR/RNase Protection Analysis

RNA from homogenized tissues (lung, kidney, heart, skeletal muscle, brain, diaphragm, and smooth muscle) was extracted using UltraspecTM (Biotecx laboratories) and analyzed essentially as described by Dennis et al. (1996).

Western Analysis

Tissues were homogenized in gel loading buffer (75 mM Tris-HCl pH 6.8; 3.8% SDS; 4 M urea; 20% glycerol) and the total protein content assessed (Biorad DC Assay kit). After addition of 5% β-mercaptoethanol and 0.001% bromophenol blue, 100 μg of each extract was separated on a polyacrylamide gel (8% for dystrophin and utrophin; 12% for β-dystroglycan) and electroblotted onto a nitrocellulose membrane. The membranes were then incubated with antibodies to utrophin (MANCHO7), or dystrophin (MANDRA1, both used at 1/100; kind gifts of Dr. G.E. Morris), or β-dystroglycan (43DAG/8D5, used at 1/10; kind gift of Dr. L.V.B. Anderson), or α-sarcoglycan (polyclonal, used at 1/50; kind gift of Dr. K.P. Campbell, Howard Hughes Medical Institute, Iowa City, IA). Bound primary antibodies were detected by horseradish peroxidase–conjugated secondary antibodies followed by chemiluminescence (Boehringer).

Histology and Immunocytochemistry

All immunolabeling was done on 6-μm thick unfixed sections of muscle, frozen in isopentane cooled in liquid nitrogen. All antibodies were applied in PBS containing 3% bovine serum albumin and 100 mM lysine for 1 h at room temperature. Primary antibodies against the following proteins were used; utrophin (G3, polyclonal affinity purified, kind gift of Dr. C.A. Sewry, London, UK; DRP1/12B6 and DRP3/20C5, monoclonals against the COOH terminus and NH_2 terminus, respectively, both used at 1/10, kind gift of Dr. L.V.B. Anderson, Newcastle, UK; MANCHO7, monoclonal against COOH terminus, used at 1/10 kind gift of Dr. G.E. Morris, MRIC Biotechnology Group, Aberystwyth, UK), dystrophin (P6, polyclonal, kind gift of Dr. C.A. Sewry, London, UK; DY8/6C5, monoclonal, used at 1/10, kind gift of Dr. L.V.B. Anderson, Newcastle, UK), dystroglycan (43DAG/8D5, monoclonal against β-dystroglycan, used at 1/100, kind gift of Dr. L.V.B. Anderson, Muscular Dystrophy Group Research Laboratory, Newcastle, UK; polyclonal against α, β-dystroglycan, kind gift of Dr. K.P. Campbell, IA), α-sarcoglycan (polyclonal, kind gift of Dr. K.P.

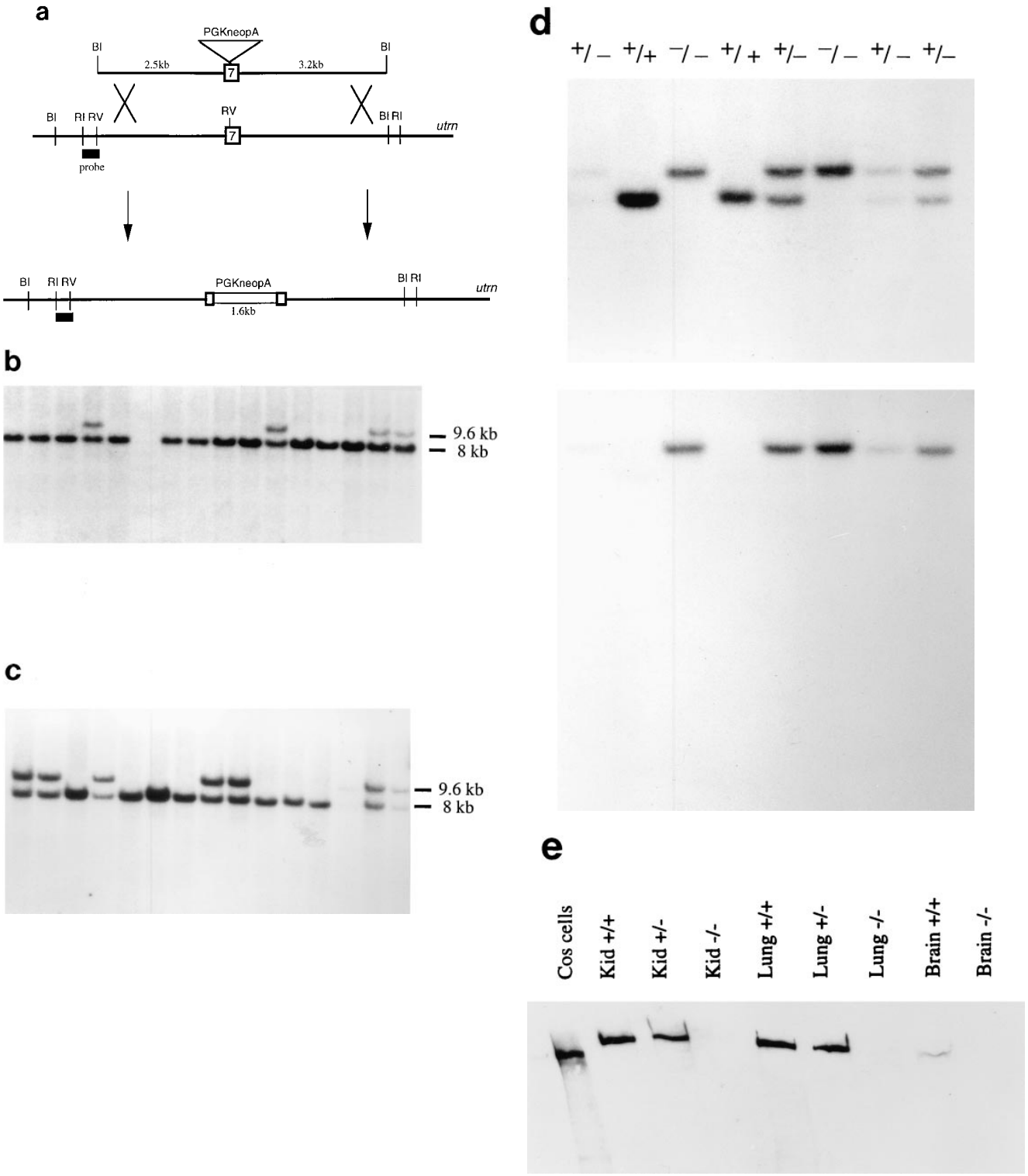

Figure 1. Production of *utrn*−/− mice. (*a*) Targeting vector, homologous genomic region with external probe region, and predicted product of the homologous recombination event. Restriction enzymes are denoted as follows: BI (BamHI); RI (EcoRI); RV (EcoRV). (*b*) Southern blot analysis of G418 resistant ES cell colonies; targeted events were identified by the presence of an additional band at 9.6 kb. (*c*) Southern blot analysis of tail biopsies from germline offspring; heterozygotes were identified by presence of targeted (9.6 kb) allele. (*d*) *Top*: breeding of heterozygotes produced Mendelian ratios of +/+ (8kb), +/− (8 kb and 9.6 kb), and −/− (9.6 kb); *bottom*: reprobing with internal *neo* probe confirms hybridization only to the 9.6-kb band. (*e*) Western blot analysis of +/+, +/−, and −/− kidney and lung and +/+, −/− brain, showing absence of utrophin in −/− tissues; COS cells used as positive control for size of utrophin (~400 kD).

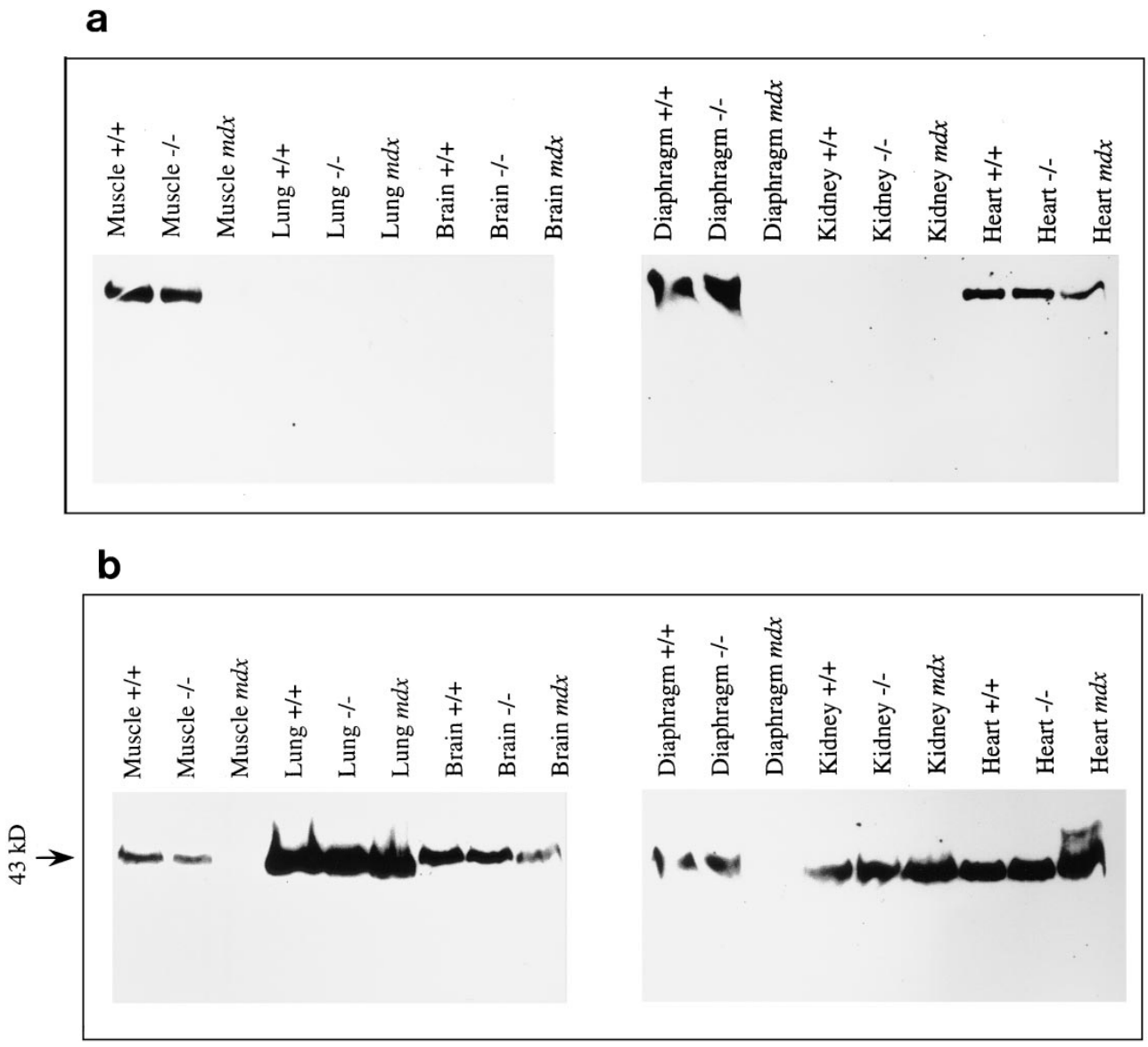

Campbell, IA), rapsyn (polyclonal raised by A. Vincent against recombinant rapsyn kindly provided by Dr. J.R. Sanes, St. Louis, MO).

Immunoreactivity was visualized using secondary antibodies conjugated with TRITC (DAKO), preincubated with normal rat serum. To identify NMJs, AChRs were labeled in the same sections with FITC-α-bungarotoxin (α-BgTx) (0.6×10^{-6} M, Molecular Probes, Eugene, OR). Labeled sections were mounted in Vectashield (Vector Labs, Burlingame, CA). Sections incubated in diluent without primary antibody served as controls for nonspecific binding of secondary antibodies. Utrophin was also labeled in teased, permeabilized SOL muscle fibers, as described by Bewick et al. (1992). Additional sections were stained with hematoxylin and eosin for histological examination.

Labeling was recorded photographically using a Leica DMRBE microscope or by a computer controlled cooled CCD camera (AstroCam 4100).

Creatine Kinase and Protein in Urine Assay

Mice were bled by tail biopsy under nonstressful conditions. 3 μl of serum was assayed for creatine kinase activity (Boehringer Mannheim MPR 1 kit). Urine was collected and assayed for protein content (Sigma Microprotein kit).

AChR Quantification

AChR abundance was estimated from α-BgTx binding which was assessed in two ways; from radioactive α-BgTx binding and from the intensity of fluorescent α-BgTx labeling.

To assess binding of radiolabeled α-BgTx, freshly dissected muscles were incubated in ^{125}I-α-BgTx (200 μCi/mM, Amersham), at a concentration of 0.5×10^{-8} M in Liley's solution (Liley, 1956) for 4 h at 20–22°C and then washed. The muscles were then fixed (5% glutaraldehyde in 0.1 M phosphate buffer, pH 7.2 for 1.5 h) and washed overnight at 4°C. Adult muscles (diaphragm, DIA; *soleus*, SOL; *extensor digitorum longus*, EDL; *epitrochleoanconeus*, ETA) were teased into bundles of 10–20 fibers and reacted to demonstrate AChE activity (Karnowsky and Roots, 1964). Regions of the bundles containing NMJs were cut out along with an adjacent piece, free of NMJs, of the same length. The pieces (15 pairs per muscle) were mounted on slides and the number of NMJs in each piece counted under the microscope. Separate pools were made of pieces with or without NMJs and the total radioactivity in each pooled sample was determined in a γ counter. At least two muscles of each type were analyzed and the results averaged. For younger mice, the small and closely packed NMJs could not be accurately counted. Hemidiaphragms with ribs attached were incubated in ^{125}I-α-BgTx, washed extensively, fixed, and reacted to demonstrate AChE activity as described above. Regions of diaphragms containing NMJs were then cut out with an adjacent, NMJ-free, piece of the same length for radioactive counting. NMJ-specific ^{125}I-α-BgTx binding for each hemidiaphragm was determined after subtracting non-NMJ binding per unit weight.

To determine the intensity of fluorescent α-BgTx labeling, muscles

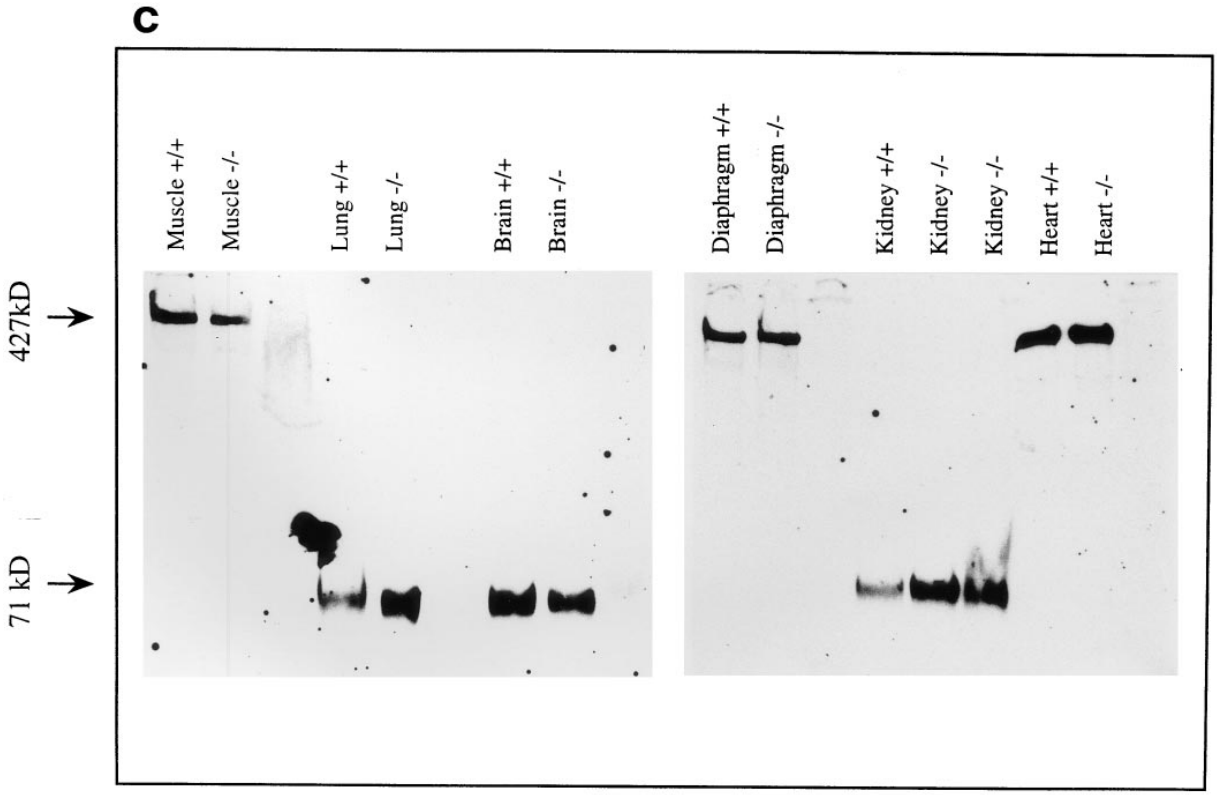

Figure 2. Western analysis. Western analysis of wild-type and *utrn*−/− skeletal muscle, lung, brain, diaphragm, kidney, and heart showing normal levels of α-sarcoglycan (*a*) and β-dystroglycan (*b*), while reduced in *mdx* muscles. Dystrophin levels in *utrn*−/− tissues appear similar to those of wild-type tissues (*c*). The 71-kD protein is one of the shorter alternative dystrophin transcripts (Dp71) which is present at high levels in nonmuscle tissues.

were incubated for 4 h at 20–22°C in TRITC-α-BgTx (Molecular Probes) at a concentration of 0.6×10^{-6} M in Liley's solution. After washing, the labeled muscles were fixed in 1% paraformaldehyde for 30 min, washed, teased into small bundles, and mounted in Vectashield. The samples were viewed in a fluorescence microscope and digitized images recorded using a 50 × objective with a cooled CCD camera (AstroCam 4100) for analysis using IMAGER2/Visilog software. After thresholding by eye to define the region of high AChR density at each NMJ, the area and average intensity of fluorescence in the selected region were obtained.

Demonstration of AChE Activity and Intramuscular Nerves

Muscles (DIA, SOL, EDL, and ETA) were fixed in 4% paraformaldehyde and then reacted to demonstrate AChE activity (Karnovsky and Roots, 1964). Teased single fibers were then mounted on slides for observation. To visualize motor axons, some samples were then further stained using a slightly modified version of the silver impegnation method of Tsuji and Tobin-Gros (1980). Further details are given in Slater et al. (1992).

Ultrastructural Analysis

For ultrastructural studies, including localization of AChRs, fresh muscles (DIA, SOL, EDL, and ETA) were incubated for 4 h (room temperature) in biotin-α-BgTx (2.4×10^{-6} M, Molecular Probes) in Liley's solution and washed before fixing in 2.5% glutaraldehyde in 0.1 M phosphate buffer, pH 7.2 for 1.5 h on ice. Small bundles of fixed muscle fibers were reacted with a streptavidin/biotin/HRP complex (DAKO) for 1 h and then reacted with 3′, 3′-diaminobenzidine with H_2O_2. Small blocks containing NMJs were then processed for electron microscopy as described by Slater et al. (1992).

The spatial frequency of postsynaptic folds ('openings/μm,' Table II) was determined by counting the number of fold openings in the region of the muscle fiber surface immediately underlying the nerve terminal and dividing this number by the length of the region of close nerve-muscle contact.

Neuromuscular Transmission

Neuromuscular transmission was assessed in detail in isolated EDL nerve-muscle preparations from mice aged 6–8 wk. Preparations were maintained in gassed (95% O_2–5% CO_2) Liley's solution at 20–22°C. Muscle fiber action potentials were blocked by exposure to 10^{-6} M μ-conotoxin, GIIIB (Peptide Institute, Inc., Osaka, Japan). Two intracellular microelectrodes were placed in each muscle fiber in the vicinity of the NMJs. The membrane potential was maintained at −75 mV by passing current through one electrode while recording voltage with the other. Endplate potentials were evoked by nerve stimulation (1 Hz) and recordings were only made if the risetime (10–90%) of the endplate potentials was < 1 ms, indicating proximity to the NMJ. At most NMJs studied, about 50 spontaneous miniature endplate potentials and 50 nerve-evoked (supramaximal stimulation at 1 Hz) endplate potentials were recorded and then a similar number of miniature endplate currents and evoked endplate currents were recorded using a two-electrode voltage clamp arrangement (holding potential −75 mV). The features of these recordings in Table III were determined using software provided by John Dempster (Strathclyde, UK). Quantal content was determined from the ratio of the mean values of the endplate currents and miniature endplate currents at each NMJ. Studies of miniature endplate potentials were also made in isolated diaphragm preparations from mice ranging from 21–56-d-old.

Statistics

All tests for differences of mean values were made with two-tailed Student's *t* test.

Results

Generation of Utrophin-Deficient Mice

A clone containing utrophin exon 7 (by analogy to dystro-

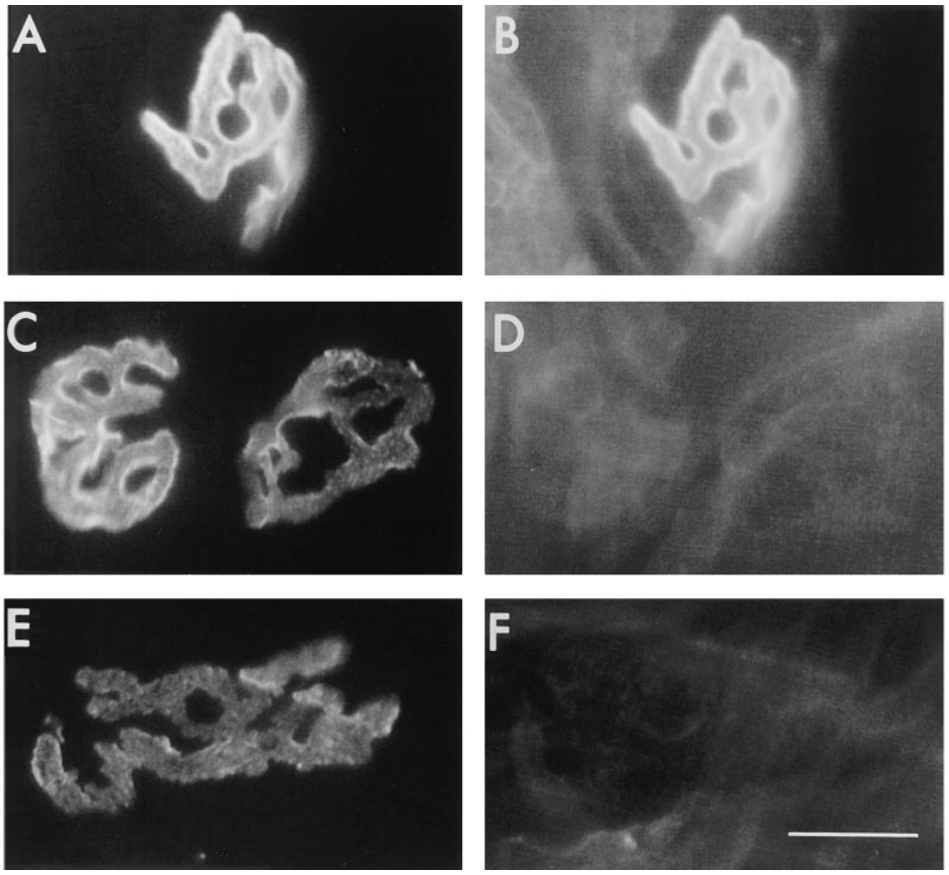

Figure 3. Utrophin is absent at the NMJ in *utrn*−/− mice. NMJs on permeabilized whole SOL muscle fibers. (*A* and *B*) wild type; (*C–F*) *utrn*−/−; (*A*, *C*, and *E*) AChRs labeled with FITC-α-BgTx; (*B* and *D*) utrophin labeled with antibody DRP3/20C5; (*F*) no primary antibody. At NMJs from *utrn*−/− mice, although AChR labeling is present, no utrophin labeling can be seen. Bar, 20 μm.

phin) flanked by 7 kb of intronic sequence was obtained from a mouse 129/Sv library. A 5′-end fragment was removed for use as an external genomic probe in Southern analysis and a neomycin cassette was introduced into the exon to disrupt the reading frame (Fig. 1 *a*). Targeted R1 ES cell lines were obtained at a frequency of ~10% (Fig. 1 *b*). Chimeras were generated to produce mice heterozygous for the mutation (Fig. 1 *c*). Breeding resulted in Mendelian ratios of wild type, heterozygotes, and homozygote mice (Fig. 1 *d*). RT PCR analysis suggested aberrant splicing of the targeted exon, with RNase protection assays demonstrating significantly decreased utrophin mRNA levels in the knockout mice (data not shown). Western analysis of kidney, lung, and brain, the tissues in which utrophin is normally most abundant, confirmed that utrophin is absent in the homozygotes (Fig. 1 *e*), a result confirmed by immunocytochemical analysis (see below). The utrophin knockout mice are referred to as *utrn*−/− mice. Since the mutation is in the actin-binding domain, these mice do not have altered expression of any shorter COOH-terminal transcripts, such as G-utrophin (Blake et al., 1995).

Phenotype of the utrn−/− Mice

In spite of the apparently complete absence of utrophin, no phenotypic abnormalities were seen in *utrn*−/− mice. The newborn mice were of normal size and appearance, suggesting that embryonic development had proceeded normally. They ate and gained weight normally after birth and have remained indistinguishable from wild type and heterozygote litter mates to date (8 mo). There were no signs of abnormal breathing or locomotor behavior and no indication of muscle weakness in the *utrn*−/− mice. The mutant mice bred and reproduced at least as well as the inbred C57BL6/J strain from which they were partially derived, suggesting that lack of utrophin does not affect smooth muscle function involved in reproduction.

Histological examination of various tissues revealed no obvious morphological abnormalities, even in kidney and lung where utrophin is normally very highly expressed. To check whether lack of utrophin caused defects in the glomerular filtration barrier, the level of protein in urine was determined. Utrophin deficient mice did not show increased protein levels in urine, suggesting that kidney function is normal. Creatine kinase levels in the serum of mice over three weeks old were normal, suggesting that there is no degeneration of cardiac or skeletal muscle.

Western Analysis of utrn−/− Mice

As described above, utrophin was undetectable by Western blotting in the tissues studied (Fig. 1 *e*). To analyze the effect of loss of utrophin on other members of the DPC, levels of α-sarcoglycan and β-dystroglycan were studied in various tissues. In muscle, α-sarcoglycan and β-dystroglycan were present at similar levels in wild-type and *utrn*−/− mice (Fig. 2, *a* and *b*), while reduced in *mdx* muscles. β-Dystroglycan was also present at similar levels in *utrn*−/− and wild-type lung, kidney, brain, and heart (Fig. 2 *b*).

To see whether upregulation of dystrophin could account for the lack of phenotype observed in *utrn*−/− mice, dystrophin levels were compared to those in wild-type

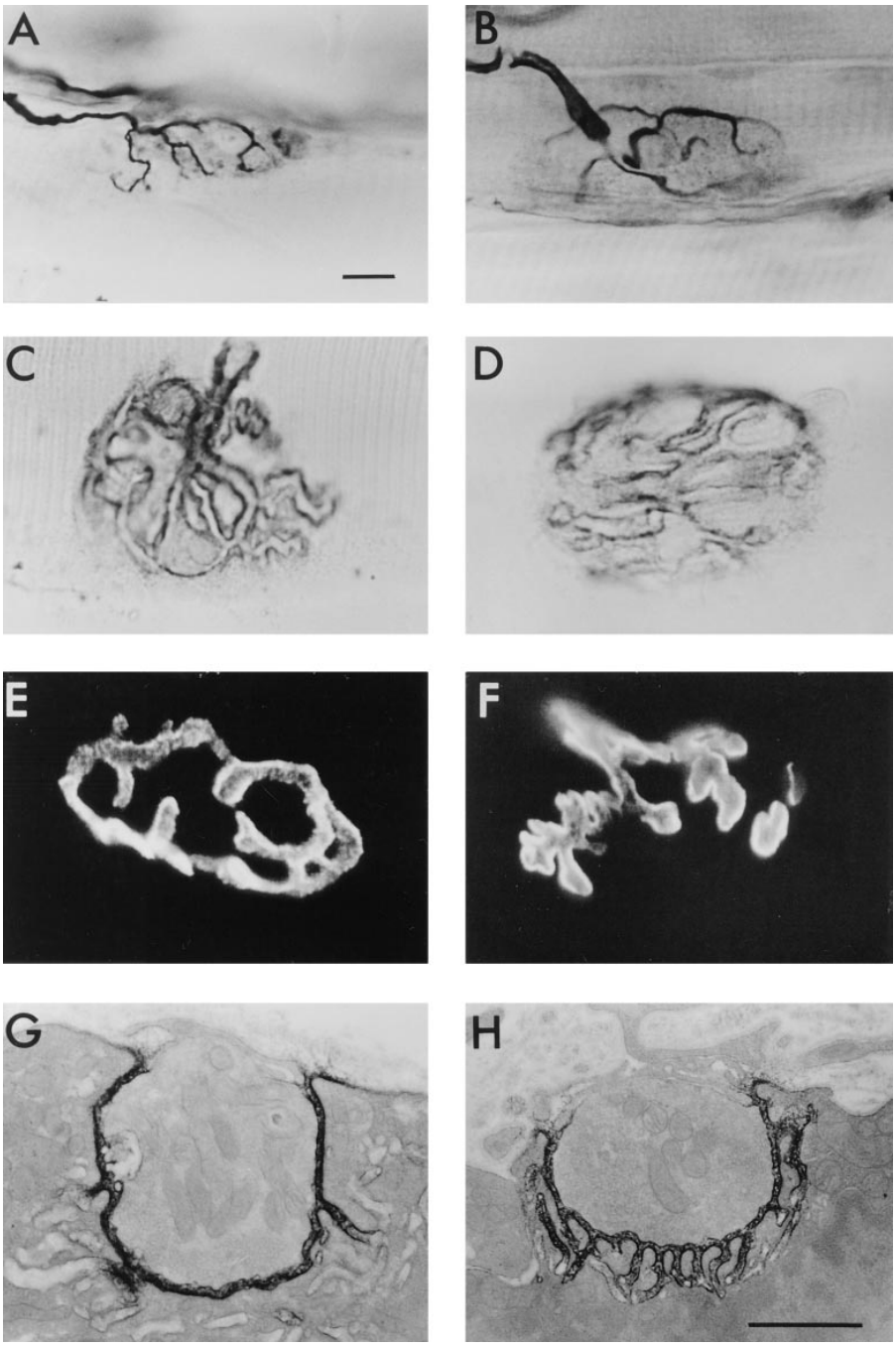

Figure 4. Structure of the NMJ in *utrn*−/− and wild-type soleus muscles. (*A*, *C*, *E* and *G*) *utrn*−/− mice; (*B*, *D*, *F*, and *H*) wild type. (*A* and *B*) Motor axon terminals, impregnated with silver, show no preterminal or ultraterminal sprouting. (*C* and *D*) AChE, demonstrated by a histochemical method, is well localized to the region of nerve contact. (*E* and *F*) AChRs, labeled with TRITC-α-BgTx, are highly concentrated in the postsynaptic region. (*g* and *h*), AChRs, labeled with HRP-avidin-biotin-α-BgTx, are concentrated in the postsynaptic membrane at the crests of the folds. Note that the number of fold openings is much less at the *utrn*−/− NMJ than in the wild type. Bars: (*A–F*) 20 μm; (*G* and *H*) 1 μm.

mice. No increase in dystrophin abundance in *utrn*−/− mice was seen in skeletal muscle, heart, or brain (Fig. 2 *c*). However, the low abundance of utrophin in these tissues implies that a low increase in dystrophin levels could be sufficient and thus be undetected by Western analysis.

Structure of the Neuromuscular Junction

Immunocytochemical labeling studies were made to confirm the absence of utrophin at the NMJ of *utrn*−/− mice. In these studies, FITC-α-BgTx was used to identify the NMJs on teased single soleus muscle fibers, labeled after permeabilization with an antibody against the NH_2-terminal of utrophin (Fig. 3). In wild-type muscles, utrophin was clearly labeled in a pattern essentially identical to that of the AChRs (Fig. 3, *A* and *B*). No labeling for utrophin could be detected at NMJs in *utrn*−/− mice (Fig. 3, *C–F*).

The general structure of the NMJ was found to be essentially normal in *utrn*−/− mice (Fig. 4). Each muscle fiber was innervated by a single motor axon which branched within the junctional zone (Fig. 4, *A* and *B*). Extrasynaptic nerve sprouts, present in a number of recently described knockout mice lacking key synaptic proteins (e.g., rapsyn, Gautam et al., 1995; agrin, Gautam et al., 1996 and MuSK, DeChiara et al., 1996) were absent. Both AChE (Fig. 4, *C* and *D*) and AChRs (Fig. 4, *E* and *F*) were highly concentrated at the NMJ and their distribution was indistinguishable from that in wild-type mice, indicating that these im-

portant molecular components of the postsynaptic surface are concentrated at the NMJ in the absence of utrophin. The size of the NMJs, as indicated by the area of the region strongly labeled by TRITC-α-BgTx, was not significantly different in *utrn*−/− and control muscles (Table I).

To determine whether the ultrastructure of NMJs lacking utrophin was normal, electron microscopic studies were made of four different muscles (DIA, SOL, EDL, and ETA). In all cases, the main ultrastructural features of normal NMJs were present, including the nerve terminal with its synaptic vesicles and mitochondria and the folded postsynaptic surface (Fig. 4, *G* and *H*). At many NMJs in *utrn*−/− mice, the postsynaptic folding appeared less extensive than that in wild-type mice, an impression that was confirmed by quantitative analysis (see below). Although utrophin is normally expressed in Schwann cells, these did not show any abnormal morphological features.

AChR Density and Folding at the Neuromuscular Junction

The abundance of AChRs at the NMJ was examined using labeled conjugates of α-BgTx (Table I). Studies with ^{125}I-α-BgTx revealed a consistent reduction in the number of α-BgTx binding sites per NMJ in *utrn*−/− mice relative to wild type in DIA, SOL, EDL, and ETA. The mean binding per NMJ, averaged from all four muscles, was 57% of that in the wild type. This reduction in the number of AChRs per NMJ could result from a reduction in the overall size of the NMJs or in the density of AChRs within the junctional region. Since there was no indication of reduced NMJ area, we tested the possibility of a reduction in AChR density by quantifying the intensity of fluorescent labeling by TRITC-α-BgTx of NMJs viewed en face in whole muscle fibers. This was very significantly reduced, relative to the wild type, in all three *utrn*−/− muscles studied (DIA, SOL, and ETA; Table I).

This reduction in the intensity of TRITC-α-BgTx labeling, seen in the light microscope, might reflect a true decrease in AChR density, i.e., in the number of AChRs/unit area of postsynaptic membrane. Alternatively, it might reflect a reduction in the amount of AChR-rich membrane within the junctional region, which could result from decreased postsynaptic folding. At wild-type NMJs, the postsynaptic membrane has infoldings occurring approximately every 0.5 μm, extending inwards for ~0.5–0.6 μm. AChRs, seen labeled with biotinylated α-BgTx followed by an electron-dense marker (Fig. 4 *G*), are highly concentrated in the crests and upper third of the folds, but virtually absent from the troughs. In the *utrn*−/− mice (Fig. 4 *H*), AChRs were also well-localized at the tops of the folds but the extent of folding appeared to be reduced. Analysis of the frequency of folds at NMJs showed that in DIA and SOL, the number of fold openings per μm of nerve-muscle contact is significantly less in *utrn*−/− mice than in wild type, although this was not true in EDL and ETA (Table II). When the data from all four muscles are pooled the frequency of fold openings at *utrn*−/− NMJs was 63% of that in controls. This was not significantly different from the fractional reduction in ^{125}I-α-BgTx bound per NMJ (57%, see above).

The previous observations suggest that the reduction in AChR abundance may be related to the decrease in folding. To test this idea further, studies of ^{125}I-α-BgTx binding were undertaken at several times during early postnatal development, before and after the folds form (Fig. 5). At birth and seven days postnatal, when little folding has developed (Matthews-Bellinger and Salepeter, 1983; Bewick et al., 1996), ^{125}I-α-BgTx binding was the same in the utrophin deficient mice as in wild type. By 21 d postnatal, when the extent of folding has nearly reached adult values, a clear difference is evident.

Neuromuscular Transmission

To assess the effect of the absence of utrophin on synaptic function, neuromuscular transmission was analyzed from intracellular recordings of spontaneous and evoked synaptic potentials and currents studied in muscle fibers in which the action potentials had been blocked with μ-conotoxin. There was no difference in the amplitude or frequency of spontaneous miniature endplate potentials in either adult (8-wk-old) EDL (Table III) or in DIA from mice 21, 38, or 56-d-old (data not shown). The amplitude of evoked endplate potentials and endplate currents and the quantal content (the number of acetylcholine quanta released from the nerve by a single nerve impulse) were all normal in the *utrn*−/− mice, suggesting that ACh release and action were normal. The decay time of the endplate currents was also normal, suggesting that the kinetics of the ACh-gated ion channels was not altered by the lack of utrophin. While many features of neuromuscular transmission were normal in *utrn*−/− mice, the amplitude of min-

Table I. α-Bungarotoxin Binding at NMJs in utrn−/− and Wild-Type Mice

	Muscle	*utrn*−/− (× 10^7 sites/NMJ)	Wild-type (× 10^7 sites/NMJ)	Ratio§ *utrn*−/− to wild-type	*P*
^{125}I-α-BgTx*	DIA	0.62, 0.80	1.01, 1.25	0.63	
	SOL	0.40, 0.56	0.84, 0.99	0.52	
	EDL	0.66	1.20	0.55	
	ETA	0.52, 1.11	1.11, 1.76	0.57	
TRITC-α-BgTx Area (μm^2)‡	DIA	356 ± 13	364 ± 13	0.98	NS
	SOL	494 ± 29	508 ± 16	0.97	NS
	ETA	423 ± 22	548 ± 33	0.77	NS
Intensity‡ (Arbitrary units)	DIA	786 ± 33	1234 ± 57	0.64	<0.0001
	SOL	701 ± 22	971 ± 31	0.72	<0.0001
	ETA	423 ± 35	562 ± 33	0.75	<0.0001

*Each value is the number of ^{125}I-α-BgTx binding sites/NMJ determined for one muscle.
‡Values are mean ± SD of a total of 20–60 NMJs in 1–3 muscles.
§Values are ratios of the mean value for *utrn*−/− NMJs to that for wild-type NMJs.

Table II. Postsynaptic Folding at the NMJs in utrn−/− and Wild-Type Mice

Muscle	*utrn*−/−* (openings/μm)	Wild type* (openings/μm)	*P*
DIA	1.15 ± 0.77 (22)	1.78 ± 0.75 (23)	<0.01
SOL	0.65 ± 0.49 (19)	2.07 ± 0.59 (21)	<0.0001
EDL	1.96 ± 1.06 (31)	2.16 ± 0.78 (13)	NS
ETA	1.21 ± 0.68 (15)	1.92 ± 1.17 (9)	NS

*Values are mean ± SD of (N) NMJs.

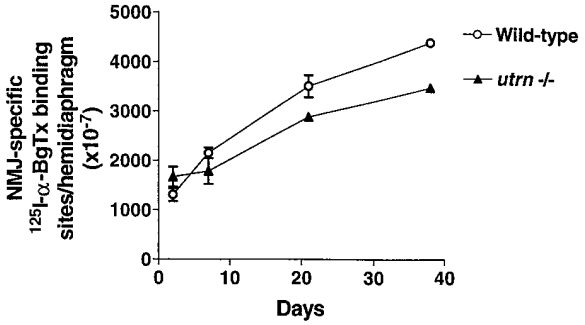

Figure 5. ^{125}I-α-BgTx binding in hemidiaphragms during postnatal development. Measurements of NMJ-specific binding per hemidiaphragm were made from individual litters of wild-type and *utrn*−/− mice at different time points and are given as mean ± SD (N = 1–4). A clear difference in α-BgTx binding between *utrn*−/− and wild-type muscles is only seen once the postsynaptic folds have formed at 21 d ($P < 0.01$, $n = 6$). At 38 d, only one hemidiaphragm was examined from each mouse, but in another litter of mice, the results were also significantly different at 49 and 56 d ($P < 0.01$ and $P < 0.05$, respectively).

iature endplate currents was reduced by 20% in EDL. This is consistent with a reduction in the density of AChRs.

Immunocytochemistry of Skeletal Muscle and NMJs

Immunofluorescence studies were made to investigate the possible effects of the absence of utrophin on the abundance of proteins normally closely associated with it in muscle and at the NMJ. Labeling of unfixed cryostat sections of wild-type DIA with antibodies to utrophin confirmed that strong utrophin immunoreactivity was present at all NMJs and absent in the extrajunctional region (Fig. 6 *A*). In contrast, no signal was seen at the NMJs from *utrn*−/− mice (Fig. 6 *F*) other than that seen in controls with no primary antibody (Fig. 6, *E* and *J*). The results illustrated were obtained with DRP1/12B6, an antibody to the COOH terminus, but similar results were obtained with DRP3/20C5, which is specific for the NH_2 terminus (see also Fig. 3). This rules out the possibility that short forms of utrophin, which include one end or the other of the whole protein, are expressed at the NMJ in *utrn*−/− mice. Labeling with antibodies to dystrophin (Fig. 6, *B* and *G*), β-dystroglycan (Fig. 6, *C* and *H*), and α-sarcoglycan (data not shown), showed normal localization of these proteins in the extrajunctional region of the muscle fiber and at the NMJ in *utrn*−/− mice. Labeling with an antibody for rapsyn was absent in the extrajunctional region and present at the NMJ in both control and *utrn*−/− muscle (Fig. 6, *D* and *I*).

Table III. Neuromuscular Transmission in the EDL Muscle of utrn−/− and Wild-Type Mice

	utrn−/−*	Wild-type*	*P*
mEPP amplitude (mV)	0.46 ± 0.18 (43)	0.51 ± 0.28 (50)	NS
mEPP frequency (Hz)	3.42 ± 2.26 (39)	3.48 ± 2.45 (47)	NS
EPP amplitude (mV)	22.6 ± 6.9 (34)	25.4 ± 7.2 (24)	NS
mEPC amplitude (mA)	2.48 ± 0.81 (35)	3.10 ± 1.02 (35)	<0.01
EPC amplitude (mA)	197.1 ± 125.8 (28)	253.3 ± 117.2 (18)	NS
EPC decay time constant (ms)	1.19 ± 0.30 (26)	1.17 ± 0.28 (18)	NS
Quantal content	81.0 ± 42.1 (26)	94.9 ± 34.6 (16)	NS

*Values are mean ± SD of data from a total of (N) NMJs, from two muscles, isolated from 8-wk-old mice. mEPP, miniature endplate potential; EPP, endplate potential; mEPC, miniature endplate current; EPC, endplate current.

Discussion

We have created mice carrying a targeted mutation at the NH_2-terminal of the utrophin gene. In studies of protein expression by Western blotting and immunocytochemistry, using antibodies to both the NH_2- and COOH-terminals, utrophin levels were undetectable in these mice, even at sites of normally high abundance such as blood vessels and the NMJ. Surprisingly, the absence of utrophin had no obvious effect on the phenotype of the *utrn*−/− mice. Nonetheless, the *utrn*−/− mice showed changes in AChR numbers and postsynaptic currents, and a highly significant reduction in postsynaptic folds. Similar observations have been made in utrophin-deficient mice in which the utrophin gene is targeted at the COOH-terminal end (Grady et al., 1997). Utrophin, like dystrophin, is thought to have many shorter isoforms, most containing either COOH-terminal or NH_2-terminal sequences (Blake et al., 1995; Nguyen thi Man et al., 1995). The similarity in the effects of targeting the COOH-terminal and NH_2-terminal regions suggests that these shorter isoforms are not essential for a normal phenotype.

In spite of its suggestive distribution within the NMJ, the absence of utrophin had remarkably little effect on the overall structure and function of the NMJ. This is in striking contrast to the devastating effects of knocking out several other postsynaptic molecules (rapsyn, Gautam et al., 1995; agrin, Gautam et al., 1996; MuSK, DeChiara et al., 1996). In particular, the localization of AChRs within the junctional region, as seen with both the light- and electron microscopes, appeared normal. Thus, in spite of its very close spatial association with the AChRs throughout development and in the adult, utrophin does not appear to be essential for AChR localization or for the development of functional NMJs, as has been suggested (Phillips et al., 1993; Campanelli et al., 1994). In view of the close association between RAPsyn and AChRs, one might expect similarly reduced levels of RAPsyn, but preliminary immunofluorescence studies show strong labeling.

While many features of the NMJs in *utrn*−/− mice were normal, two abnormalities were observed; a reduction in the number of AChRs per NMJ and a reduction in the frequency of postsynaptic infoldings. These two findings may be related. Since AChRs are particularly concentrated in the region of the folds nearest their opening onto the extracellular space, the observed reduction in the number of those openings would be expected to reduce the area of membrane available to accommodate AChRs. This view is supported by our finding that the decreased abundance of AChRs in *utrn*−/− mice is not detectable until the postsynaptic folds form during development. The process by which folds form, and the factors which may influence that process, are not understood. The decrease in the spatial frequency of folds was more obvious in diaphragm and soleus than in EDL and ETA. The former muscles are normally active either continuously (soleus) or in small bursts

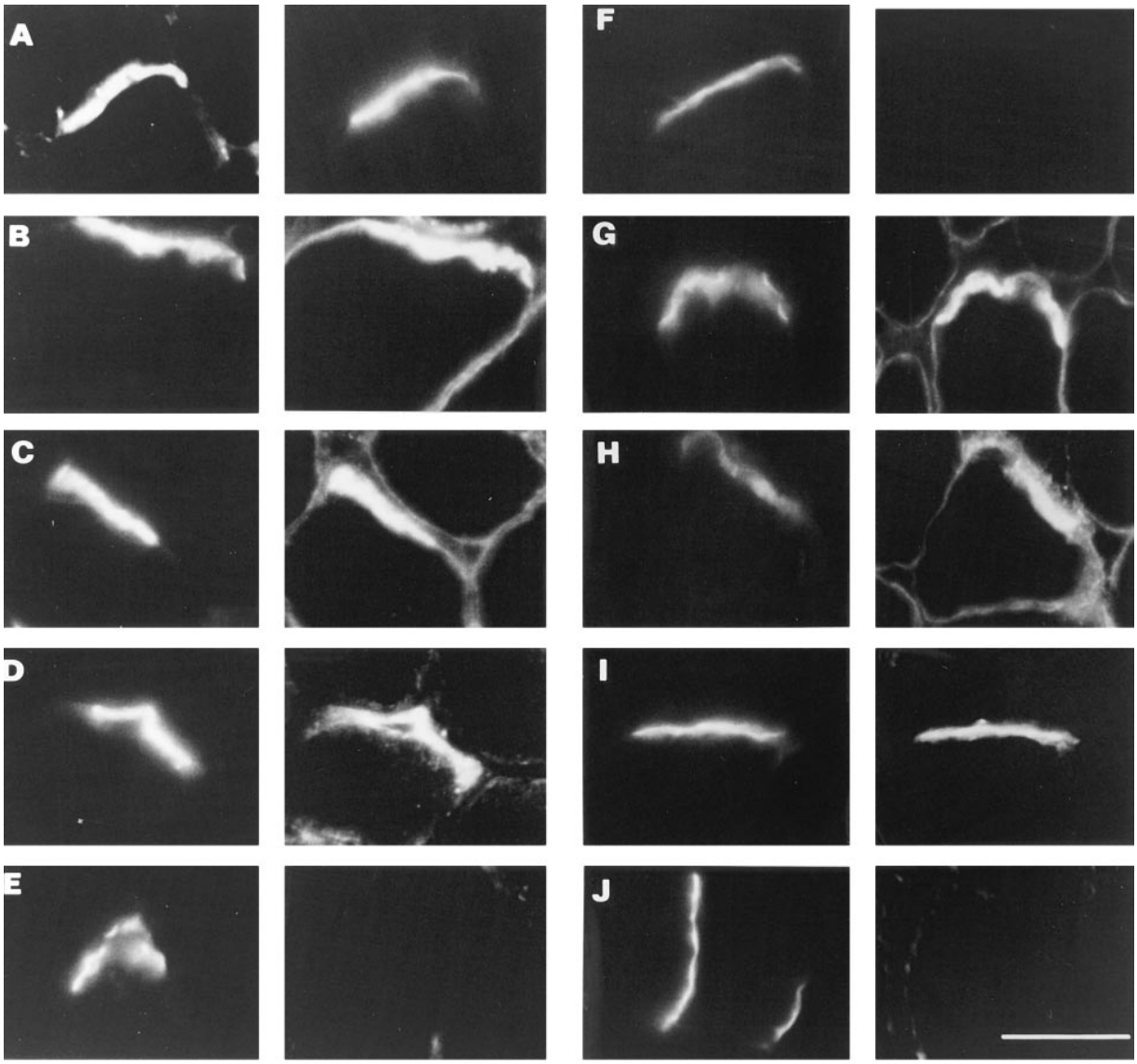

Figure 6. Postsynaptic proteins at the NMJ of wild-type and *utrn*−/− mice. Immunolabeling of transverse frozen sections, including junctional and extrajunctional regions of the surface of DIA fibers, is shown for wild-type (*A–E*) and *utrn*−/− (*F–J*) fibers. For each pair of images, the left panel shows the NMJ, labeled with FITC-α-BgTx. The right panel shows immunolabeling visualized with TRITC-conjugated second antibody. The antibodies used were (*A* and *F*) utrophin (DRP1/12B6); (*B* and *G*) dystrophin (DY8/6C5); (*C* and *H*) β-dystroglycan (43DAG/8D5); (*D* and *I*) rapsyn (rabbit polyclonal against recombinant rapsyn); (*E* and *J*) no primary antibody. While utrophin labeling is absent at *utrn*−/− NMJs, the pattern of labeling of all other antibodies is the same in *utrn*−/− and wild-type NMJs. For each antibody, the images of wild-type and *utrn*−/− NMJs have been printed under equivalent conditions. Bar, 20 μm.

related to the respiratory cycle (diaphragm) while the latter are fast twitch muscles which fire relatively infrequently and in short, high-frequency bursts (Hennig and Lømo, 1985). This suggests that the pattern of activity may have some influence on the formation or maintenance of folds. Postsynaptic folding is also reduced in *mdx* mice which lack dystrophin (Bulfield et al., 1984; Sicinski et al., 1989; Torres and Duchen, 1987; Lyons and Slater, 1991). While this may reflect a rather nonspecific effect of abnormalities of the postsynaptic cytoskeleton on the incidence of folds, it may also be that cycles of muscle fiber degeneration and regeneration, which are present in *mdx* but not *utrn*−/− mice, result in reduced folding.

The normal appearance and behavior of *utrn*−/− mice suggest that the role of utrophin, in spite of its widespread distribution, is nonessential in mouse. Alternatively, the role of utrophin may be important during old age or in response to tissue damage, for example during regeneration of muscle. Another possibility is that proteins which can compensate for the function of utrophin are upregulated. The most obvious candidate for such a compensating protein is dystrophin. However, we have so far found no evidence for increased abundance of dystrophin or a de novo appearance at sites such as blood vessels which are normally rich in utrophin. Relocalization of dystrophin to the crests of the folds can unfortunately not be investigated. Frozen sections do not allow resolution between the crest and the bottom of the junctional folds, and there are no

antibodies available that allow dystrophin to be visualized adequately by EM immunolabeling.

In muscular dystrophies resulting from decreased dystrophin abundance, both in man and in *mdx* mice, there is a parallel reduction in the abundance of many of the proteins of the DPC (Ervasti et al., 1990; Ohlendieck and Campbell, 1991; Sewry et al., 1994). In *utrn* −/− mice the two members of the DPC studied, β-dystroglycan was clearly present in lung and kidney where utrophin is normally most abundant but dystrophin is not expressed. In the absence of an upregulation of dystrophin, this suggests that utrophin is not essential for the maintenance or localization of the proteins of the DPC. Nonetheless, the possibility remains that this role can be played by isoforms of dystrophin or utrophin, not recognized by the antibodies we used, that may be present normally in these tissues or upregulated in the face of decreased utrophin abundance.

Both reduced AChR abundance and decreased postsynaptic folding are features of a number of congenital myasthenic syndromes (CMS) in man, conditions in which impairment of neuromuscular transmission leads to muscle weakness and abnormal fatiguability (reviewed in Engel et al., 1993; Shillito et al., 1993; Vincent et al., 1996). The molecular and genetic basis of this heterogeneous group of disorders is poorly understood in most cases (see Engel, 1993; Engel et al., 1996; Sine et al., 1995; Ohno et al., 1995, 1996). However, in some patients with reduced AChRs and reduced folds, there is a profound reduction in the abundance of utrophin at the NMJ, although other proteins (e.g., dystrophin and β-dystroglycan) remain concentrated in the postsynaptic region (Slater et al., 1994). While this suggests some sort of link between AChRs and utrophin, the nature of that link remains unclear.

In conclusion, the absence of utrophin in *utrn* −/− mice results in mild abnormalities at the NMJ but no other signs of an abnormal phenotype. The similarity of the changes at the NMJ to those in some forms of CMS suggest that utrophin expression should be investigated in such patients, particularly since the autosomal utrophin gene represents such a large target for mutation.

We wish to thank Derek Blake and Neil Hunter for useful discussions and critical reading of the manuscript, as well as Helen Blaber, Carina Dennis, Leslie Jacobson, Ralph Nawrotzki, Graeme Penny, Sohaila Rastan, Judith Skinner, Teresa Tang, Helen Turley, and Bill Wood for suggestions or help at various stages; Colin Hetherington (and Robert) for invaluable services at the BSU, JR Hospital, and Professor Morris and Professor Bell for access to the microinjection facilities (Oxford); John Walsh for help with the electron microscopy (Newcastle).

This work was funded by the Muscular Dystrophy Group of Great Britain and Northern Ireland, the Muscular Dystrophy Association USA, the Medical Research Council, and the Wellcome Trust.

Received for publication 7 October 1996 and in revised form 6 December 1996.

References

Ahn, A.H., and L.M. Kunkel. 1993. The structural and functional diversity of dystrophin. *Nat Genet.* 3:283–291.

Belkin, A.M., and K. Burridge. 1995. Localization of utrophin and aciculin at sites of cell-matrix and cell-cell adhesion in cultured cells. *Exp. Cell Res.* 221: 132–140.

Belkin, A.M., I.V. Klimanskaya, M.E. Lukashev, K. Lilley, D.R. Critchley, and V.E. Koteliansky. 1994. A novel phosphoglucomutase-related protein is concentrated in adherens junctions of muscle and nonmuscle cells. *J. Cell Sci.* 107:1993–2003.

Bewick, G.S., L.V. Nicholson, C. Young, E. O'Donnell, and C.R. Slater. 1992. Different distributions of dystrophin and related proteins at nerve-muscle junctions. *Neuroreport.* 3:857–860.

Bewick, G.S., C. Young, and C.R. Slater. 1996. Spatial relationships of utrophin, dystrophin, β-dystroglycan and β-spectrin to acetylcholine receptor clusters during postnatal maturation of the rat neuromuscular junction. *J. Neurocytol.* 25:367–379.

Blake, D.J., J.N. Schofield, R.A. Zuellig, D.C. Gorecki, S.R. Phelps, E.A. Barnard, Y.H. Edwards, and K.E. Davies. 1995. G-utrophin, the autosomal homologue of dystrophin Dp116, is expressed in sensory ganglia and brain. *Proc. Natl. Acad. Sci. USA.* 92:3697–3701.

Blake, D.J., J.M. Tinsley, and K.E. Davies. 1996. Utrophin: a structural and functional comparison to dystrophin. *Brain Pathology.* 6:37–47.

Bulfield, G., W.G. Siller, P.A. Wight, and K.J. Moore. 1984. X chromosome-linked muscular dystrophy (mdx) in the mouse. *Proc. Natl. Acad. Sci. USA.* 81:1189–1192.

Campanelli, J.T., S.L. Roberds, K.P. Campbell, and R.H. Scheller. 1994. A role for dystrophin-associated glycoproteins and utrophin in agrin-induced AChR clustering. *Cell.* 77:663–674.

Campbell, K.P. 1995. Three muscular dystrophies: loss of cytoskeleton-extracellular matrix linkage. *Cell.* 80:675–679.

DeChiara, T.M., D.C. Bowen, D.M. Valenzuela, M.V. Simmons, W.T. Poueymirou, S. Thomas, E. Kinetz, D.L. Compton, E. Rojas, J.S. Park, et al. 1996. The receptor tyrosine kinase MuSK is required for neuromuscular junction formation in vivo. *Cell.* 85:501–512.

Dennis, C.L., J.M. Tinsley, A.E. Deconinck, and K.E. Davies. 1996. Molecular and functional analysis of the utrophin promoter. *Nucleic Acids Res.* 24: 1646–1652.

Dickson, G., A. Azad, G.E. Morris, H. Simon, M. Noursadeghi, and F.S. Walsh. 1992. Co-localization and molecular association of dystrophin with laminin at the surface of mouse and human myotubes. *J. Cell Sci.* 103:1223–1233.

Engel, A.G. 1993. The investigation of congenital myasthenic syndromes. *Ann. NY Acad. Sci.* 681:425–434.

Engel, A.G., K. Ohno, M. Milone, H.-L. Wang, S. Nakano, C. Bouzat, J. Ned Pruit II, D.O. Hutchinson, J.M. Brengman, N. Bren, et al. 1996. New mutations in acetylcholine receptor subunit genes reveal heterogeneity in the slow-channel congenital myasthenic syndrome. *Human Molecular Genetics.* 5:1217–1227.

Ervasti, J.M., and K.P. Campbell. 1991. Membrane organization of the dystrophin-glycoprotein complex. *Cell.* 66:1121–1131.

Ervasti, J.M., and K.P. Campbell. 1993. A role for the dystrophin-glycoprotein complex as a transmembrane linker between laminin and actin. *J. Cell Biol.* 122:809–823.

Ervasti, J.M., K. Ohlendieck, S.D. Kahl, M.G. Gaver, and K.P. Campbell. 1990. Deficiency of a glycoprotein component of the dystrophin complex in dystrophic muscle. *Nature (Lond.).* 345:315–319.

Froehner, S.C., C.W. Luetje, P.B. Scotland, and J. Patrick. 1990. The postsynaptic 43K protein clusters muscle nicotinic acetylcholine receptors in Xenopus Oocytes. *Neuron.* 5:403–410.

Flucher, B.E., and M.P. Daniels. 1989. Distribution of Na+ channels and ankyrin in neuromuscular junctions is complementary to that of acetylcholine receptors and the 43 kd protein. *Neuron.* 3:163–175.

Gautam, M., P.G. Noakes, J. Mudd, M. Nichol, G.C. Chu, J.R. Sanes and J.P. Merlie. 1995. Failure of postsynaptic specialization to develop at neuromuscular junctions of rapsyn-deficient mice. *Nature (Lond.).* 377:232–236.

Gautam, M., P.G. Noakes, L. Moscoso, F. Rupp, R.H. Scheller, J.P. Merlie, and J.R. Sanes. 1996. Defective neuromuscular synaptogenesis in agrin-deficient mutant mice. *Cell.* 85:525–535.

Grady, R.M., J.P. Merlie, J.R. Sanes. Subtle neuromuscular defects in utrophin-deficient mice. *J. Cell Biol.* 136:871–882.

Helliwell, T.R., N.T. Man, G.E. Morris, and K.E. Davies. 1992. The dystrophin-related protein, utrophin, is expressed on the sarcolemma of regenerating human skeletal muscle fibres in dystrophies and inflammatory myopathies. *Neuromuscul. Disord.* 2:177–184.

Hennig, R., and T. Lømo. 1985. Firing patterns of motor units in normal rats. *Nature (Lond.).* 314:164–166.

Hoffman, E.P., R.J. Brown, and L.M. Kunkel. 1987. Dystrophin: the protein product of the Duchenne muscular dystrophy locus. *Cell.* 51:919–928.

Ibraghimov-Beskrovnaya, O., J.M. Ervasti, C.J. Leveille, C.A. Slaughter, S.W. Sernett, and K.P. Campbell. 1992. Primary structure of dystrophin-associated glycoproteins linking dystrophin to the extracellular matrix. *Nature (Lond.).* 355:696–702.

James, M., N.T. Man, C.J. Wise, G.E. Jones, and G.E. Morris. 1996. Utrophin-dystroglycan complex in membranes of adherent cultured cells. *Cell Motil. Cytoskeleton.* 33:163–174.

Kamakura, K., Y. Tadano, M. Kawai, S. Ishiura, R. Nakamura, K. Miyamoto, N. Nagata, and H. Sugita. 1994. Dystrophin-related protein is found in the central nervous system of mice at various developmental stages, especially at the postsynaptic membrane. *J. Neurosci. Res.* 37:728–734.

Karnowsky, M.J., and L. Roots. 1964. Direct colouring thiocholine method for cholinesterases. *J. Cell Biol.* 23:217–223.

Karpati, G., S. Carpenter, G.E. Morris, K.E. Davies, C. Guerin, and P. Holland. 1993. Localization and quantitation of the chromosome 6-encoded dystrophin-related protein in normal and pathological human muscle. *J. Neuro-*

pathol. Exp. Neurol. 52:119–128.
Khurana, T.S., S.C. Watkins, P. Chafey, J. Chelly, F.M. Tome, M. Fardeau, J.C. Kaplan, and L.M. Kunkel. 1991. Immunolocalization and developmental expression of dystrophin related protein in skeletal muscle. *Neuromuscul. Disord.* 1:185–194.
Khurana, T.S., S.C. Watkins, and L.M. Kunkel. 1992. The subcellular distribution of chromosome 6-encoded dystrophin-related protein in the brain. *J. Cell Biol.* 119:357–366.
Koenig, M., A.P. Monaco, and L.M. Kunkel. 1988. The complete sequence of dystrophin predicts a rod-shaped cytoskeletal protein. *Cell.* 53:219–226.
Koga, R., S. Ishiura, M. Takemitsu, K. Kamakura, T. Matsuzaki, K. Arahata, I. Nonaka, and H. Sugita. 1993. Immunoblot analysis of dystrophin-related protein (DRP). *Biochim. Biophys. Acta.* 1180:257–261.
Liley, A.W. 1956. An investigation of spontaneous activity at the neuromuscular junction of the rat. *J. Physiol.* 132:650–666.
Love, D.R., D.F. Hill, G. Dickson, N.K. Spurr, B.C. Byth, R.F. Marsden, F.S. Walsh, Y.H. Edwards, and K.E. Davies. 1989. An autosomal transcript in skeletal muscle with homology to dystrophin. *Nature (Lond.).* 339:55–58.
Love, D.R., G.E. Morris, J.M. Ellis, U. Fairbrother, R.F. Marsden, J.F. Bloomfield, Y.H. Edwards, C.P. Slater, D.J. Parry, and K.E. Davies. 1991. Tissue distribution of the dystrophin-related gene product and expression in the mdx and dy mouse. *Proc. Natl. Acad. Sci. USA.* 88:3243–3247.
Lyons, P.R., and C.R. Slater. 1991. Structure and function of the neuromuscular junction in young adult *mdx* mice. *J. Neurocytol.* 20:969–981.
Matsumura, K., J.M. Ervasti, K. Ohlendieck, S.D. Kahl, and K.P. Campbell. 1992. Association of dystrophin-related protein with dystrophin-associated proteins in mdx mouse muscle. *Nature (Lond.).* 360:588–591.
Matsumura, K., H. Yamada, T. Shimizu, and K.P. Campbell. 1993. Differential expression of dystrophin, utrophin and dystrophin-associated proteins in peripheral nerve. *FEBS Lett.* 334:281–285.
Matthews-Bellinger, J.A., and M.M. Salpeter. 1983. Fine structural distribution of acetylcholine receptors at developing mouse neuromuscular junctions. *J. Neurosci.* 3:644–657.
Nguyen, t.M., J.M. Ellis, D.R. Love, K.E. Davies, K.C. Gatter, G. Dickson, and G.E. Morris. 1991. Localization of the DMDL gene encoded dystrophin-related protein using a panel of nineteen monoclonal antibodies: presence at neuromuscular junctions, in the sarcolemma of dystrophic skeletal muscle, in vascular and other smooth muscles, and in proliferating brain cell lines. *J. Cell Biol.* 115:1695–1700.
Nguyen, t.M., T.R. Helliwell, C. Simmons, S.J. Winder, J.J. Kendrick, K.E. Davies, and G.E. Morris. 1995. Full-length and short forms of utrophin, the dystrophin-related protein. *FEBS Lett.* 358:262–266.
Ohlendieck, K., and K.P. Campbell. 1991. Dystrophin-associated proteins are greatly reduced in skeletal muscle from mdx mice. *J. Cell Biol.* 115:1685–1694.
Ohlendieck, K., J.M. Ervasti, K. Matsumura, S.D. Kahl, C.J. Leveille, and K.P. Campbell. 1991. Dystrophin-related protein is localized to neuromuscular junctions of adult skeletal muscle. *Neuron.* 7:499–508.
Ohno, K., D.O. Hutchinson, M. Milone, J.M. Brengman, C. Bouzat, S.M. Sine, and A.G. Engel. 1995. Congenital myasthenic syndrome caused by prolonged acetylcholine receptor channel openings due to a mutation in the M2 domain of the epsilon subunit. *Proc. Natl Acad. Sci. USA.* 92:758–762.
Ohno, K., H.-L. Wang, M. Milone, N. Bren, J.M. Brengman, S. Nakano, P. Quiram, J. Ned Pruit II, S.M. Sine, and A.G. Engel. 1996. Congenital myasthenic syndrome caused by decreased agonist binding affinity due to a mutation in the acetylcholine receptor epsilon subunit. *Neuron.* 17:163–175.
Papaioannou, V., and R. Johnson. 1993. *In* Gene Targeting: A Practical Approach. A.L. Joyner, editor. IRL Press, Oxford. 107–146.
Pearce, M., D.J. Blake, J.M. Tinsley, B.C. Byth, L. Campbell, A.P. Monaco, and K.E. Davies. 1993. The utrophin and dystrophin genes share similarities in genomic structure. *Hum. Mol. Genet.* 2:1765–1772.
Phillips, W.D., C. Kopta, P. Blount, P.D. Gardner, J.H. Steinbach, and J.P. Merlie. 1991. ACh receptor-rich membrane domains organized in fibroblasts by recombinant 43-kDa protein. *Science (Wash. DC).* 251:568–570.
Phillips, W.D., P.G. Noakes, S.L. Roberds, K.P. Campbell, and J.P. Merlie. 1993. Clustering and immobilization of acetylcholine receptors by the 43-kD protein: a possible role for dystrophin-related protein. *J. Cell Biol.* 123:729–740.
Pons, F., A. Robert, E. Fabbrizio, G. Hugon, J.C. Califano, J.A. Fehrentz, J. Martinez, and D. Mornet. 1994. Utrophin localization in normal and dystrophin-deficient heart. *Circulation.* 90:369–374.
Schofield, J., D. Houzelstein, K. Davies, M. Buckingham, and Y.H. Edwards. 1993. Expression of the dystrophin-related protein (utrophin) gene during mouse embryogenesis. *Dev. Dyn.* 198:254–264.
Sealock, R., M.H. Butler, N.R. Kramarcy, K.X. Gao, A.A. Murnane, K. Douville, and S.C. Froehner. 1991. Localization of dystrophin relative to acetylcholine receptor domains in electric tissue and adult and cultured skeletal muscle. *J. Cell Biol.* 113:1133–1144.
Sewry, C.A., K. Matsumura, K.P. Campbell, and V. Dubowitz. 1994. Expression of dystrophin-associated glycoproteins and utrophin in carriers of Duchenne muscular dystrophy. *Neuromuscul. Disord.* 4:401–409.
Shillito, P., A. Vincent, and D.J. Newsom. 1993. Congenital myasthenic syndromes. *Neuromuscul. Disord.* 3:183–190.
Sicinski, P., Y. Geng, C.A. Ryder, E.A. Barnard, M.G. Darlison, and P.J. Barnard. 1989. The molecular basis of muscular dystrophy in the mdx mouse: a point mutation. *Science (Wash. DC).* 244:1578–1580.
Sine, S.M., K. Ohno, C. Bouzat, A. Auerbach, M. Milone, J.N. Pruitt, and A.G. Engel. 1995. Mutation of the acetylcholine receptor α subunit causes a slow-channel myasthenic syndrome by enhancing agonist binding affinity. *Neuron.* 15:229–239.
Slater, C.R., P.R. Lyons, T.J. Walls, P.R. Fawcett, and C. Young. 1992. Structure and function of neuromuscular junctions in man: a motor end point biopsy study in two patient groups. *Brain.* 115:451–478.
Slater, C.R., et al. 1994. Reduction of utrophin associated with acetylcholine receptor deficiency at the neuromuscular junction in human diseases. *J. Cell. Biochem.* 18:180.
Tinsley, J.M., D.J. Blake, A. Roche, U. Fairbrother, J. Riss, B.C. Byth, A.E. Knight, J.J. Kendrick, G.K. Suthers, et al. 1992. Primary structure of dystrophin-related protein. *Nature (Lond.).* 360:591–593.
Tinsley, J.M., D.J. Blake, R.A. Zuellig, and K.E. Davies. 1994. Increasing complexity of the dystrophin-associated protein complex. *Proc. Natl. Acad. Sci. USA.* 91:8307–8313.
Torres, L.F., and L.W. Duchen. 1987. The mutant *mdx*: inherited myopathy in the mouse. Morphological studies of nerves, muscles and end-plates. *Brain.* 110:269–299.
Tsuji, S., and C. Tobin-Gros. 1980. A simple silver nitrate impregnation of nerve fibres with preservation of acetylcholinesterase activity at the motor end-plate. *Experientia.* 36:1317–1319.
Vincent, A., C. Newland, R. Croxen, and D. Beeson. 1996. Genes at the junction—candidates for congenital myasthenic syndromes. *TINS.* 20:15–22.
Winder, S.J., and J. Kendrick-Jones. 1995. Calcium/calmodulin-dependent regulation of the NH-2-terminal F-actin binding domain of utrophin. *FEBS Letts.* 357:125–128.
Winder, S.J., L. Hemmings, S.K. Maciver, S.J. Bolton, J.M. Tinsley, K.E. Davies, D.R. Critchley, and J. Kendrick-Jones. 1995. Utrophin actin binding domain: analysis of actin binding and cellular targeting. *J. Cell Sci.* 108:63–71.
Wurst, W., and A. Joyner. 1993. In Gene Targeting: A Practical Approach. A.L. Joyner, editor. IRL Press, Oxford. 33–61.